International Journal of Neural Systems


# CAUSAL COUPLING BETWEEN ELECTROPHYSIOLOGICAL SIGNALS, CEREBRAL HEMODYNAMICS AND SYSTEMIC BLOOD SUPPLY OSCILLATIONS IN MAYER WAVE FREQUENCY RANGE

**P. LACHERT[1], J. ZYGIEREWICZ[2], D. JANUSEK[1], P. PULAWSKI[1], P. SAWOSZ[1], M. KACPRZAK[1], A. LIEBERT[1], K.J. BLINOWSKA[1,2*]**

*[1]Department of Methods of Brain Imaging and Functional Research of Nervous System, Nalecz Institute of Biocybernetics and Biomedical Engineering Polish Academy of Sciences, Ks. Trojdena 4, 02-109 Warsaw, Poland*

*[2]Department of Biomedical Physics, Faculty of Physics, University of Warsaw, Pasteura 5, 02-093, Warsaw, Poland*
**kjbli@fuw.edu.pl*

The aim of the study was to assess causal coupling between neuronal activity, microvascular hemodynamics and blood supply oscillations in the Mayer wave frequency range. An electroencephalogram, cerebral blood oxygenation changes, an electrocardiogram and blood pressure were recorded during rest and during a movement task. Causal coupling between them was evaluated using Directed Transfer Function, a measure based on the Granger causality principle. The Multivariate Autoregressive Model was fitted to all the signals simultaneously, which made it possible to construct a complete scheme of interactions between the considered signals. The obtained pattern of interactions in the resting state estimated in the 0.05-0.15 Hz band revealed a predominant influence of blood pressure oscillations on all the other variables. Reciprocal connections between blood pressure and heart rate variability time series indicated the presence of feedback loops between these signals. During movement, the pattern of connections did not change dramatically. The number of connections decreased, but the couplings between blood pressure and heart rate variability signal were not significantly changed, and the strong influence of the decreased blood hemoglobin concentration on the oxygenated hemoglobin concentration persisted. For the first time our results provided a comprehensive scheme of interactions between electrical and hemodynamic brain signals, heart rate and blood pressure oscillations. Persistent reciprocal connections between blood pressure and heart rate variability time series suggest possible feedforward and feedback coupling of cardiovascular variables which may lead to the observed oscillations in Mayer wave range.

*Keywords*: neurovascular coupling; electroencephalogram; functional near infrared spectroscopy, causal coupling; Directed Transfer Function; Granger causality.

## 1. Introduction

Slow oscillations of frequency around 0.1 Hz were detected in different electrophysiological and hemodynamic signals; however, the relations between them are still elusive. Oscillations of blood pressure around 0.1 Hz were first reported in the 19th century by Sigmund Mayer,[1] and hence are called Mayer waves (MW). Interestingly, LFOs, low frequency oscillations (0.05-0.15 Hz) centered around 0.1 Hz, were also observed in heart rate variability signal[2,3,4] and blood oxygenation levels.[5,6,7] There is also evidence that they may modulate the amplitude of EEG (electroencephalogram) rhythms.[8,9,10]

It is presumed that MW result from an oscillation of sympathetic vasomotor tone and are coupled with synchronous oscillations of efferent sympathetic nervous activity. Their amplitudes possibly reflect vascular sympathetic activity since they are most visible in response to sympathoexcitatory stimuli. MW were also observed in animals with frequencies dependent on species. A significant correlation of blood pressure with sympathetic nervous activity measured from the peroneal nerve (in humans) or from the measurement of

*Corresponding author.

renal sympathetic activity (in animals) indicates a connection between the sympathetic system and MW. Two mechanisms of generating MW were proposed.[11] One theory associates generation of MW with an autonomous oscillator located either in the brainstem or in the spinal cord. This pacemaker theory is based on the observation that the oscillations of sympathetic nervous activity and hemodynamic variables near the frequency of MW were found in the absence of sensory inputs from the periphery. However, the results from animal acute experiments and studies on patients with spinal cord injuries were not conclusive, and, even if the pacemaker of MW was actually operating, its feedforward effect on arterial pressure would necessarily be modulated by baroreflex response.[11]

The baroreflex theory is strongly supported by evidence that opening the baroreflex loop abolishes the generation of MW.[2,3] The models of dynamic arterial pressure control aiming to predict MW assume that numerous dynamic components and time delays present in the baroreflex loop would produce resonant self-sustained oscillations.[11]

However, recent publications consider the possible involvement of the central nervous system in the generation of 0.1 Hz oscillations.[12,13] An interesting problem drawing attention of researchers is the relations of LFOs occurring in different neurovascular signals, since information gained from such studies may help to understand the mechanisms of neurovascular control.

In the studies devoted to that problem, coherence analysis was usually applied.[6,9,10,14] However, coherence is a bivariate measure, so only two signals at a time can be considered. The analysis involves estimation of time delays from phase differences of selected frequencies. However, the variability of phases across the time scale makes the estimation of time shifts difficult.[10] Moreover, from coherence analysis, it is not possible to find reciprocal connections between time series and the existence of such connections is highly probable because of the presumed feedback loops in vascular and hemodynamic systems.

The choice of method for estimating the interactions between the signals of interest is of primary importance. It should be robust with respect to noise and free from the common drive effect. It should also be able to estimate effective (causal) connectivity and enable the identification of reciprocal connections. The Directed Transfer Function (DTF)[15] based on the Multivariate Autoregressive Model fulfills these requirements. DTF is a linear method and we cannot exclude non-linearities in the investigated system; however, it was demonstrated in[16] that DTF performs quite well even for non-linear signals. On the other hand, non-linear measures of connectivity are bivariate (hence, due to the common feeding effect, they may produce false connections), they are very sensitive to noise and prone to systematic errors related to the choice of parameters, e.g., the embedding dimension or bin lengths and they do not allow identification of reciprocal connections.[17,18,19] The non-linear methods require long stationary data segments (embedding procedure, construction of histograms) which makes them unsuitable for short signal segments. DTF is robust to noise[15] and the common feeding effect.[20,21] As an extension of the Granger causality principle[22], it is capable of showing causal directed interactions between signals and also allows determination of reciprocal causal interactions as functions of frequency. DTF has been widely applied for the estimation of EEG, ECoG and LFP connectivity patterns[17,18] and used for finding relations between signals of different origin.[23]

Herein we applied DTF for estimation of relations between LFOs occurring in systolic and diastolic blood pressure (sBP/dBP), heart rate variability (HRV), changes in concentration of blood oxygenation (HbO) and deoxygenation (HbR) and amplitudes of the EEG alpha and beta rhythms during awake rest and during a motor task. The aim of our investigation was to find causal relations between the above-mentioned time series in order to gain a better understanding of the interrelations between the systems involved in generation of these signals and the generation of MW, as well as elucidate their role in vascular, hemodynamic and nervous systems interactions.

## 2. Experiment design

### 2.1. *Subjects*

Eighteen subjects took part in the experiment. Subjects were treated in strict compliance with the Declaration of Helsinki. All subjects were informed about the experimental procedures and gave a written consent. The experiment was approved by the Ethical Review Board at the Medical University of Warsaw. Eight persons were excluded from the further evaluation because of their too weak or too noisy functional Near

Infrared Spectroscopy (fNIRS) signal or because of artifact abundance. fNIRS signal strength largely depends on the anatomical structure of the head, e.g., in subjects with optically-thick skulls, the signal is strongly damped.[24] However, for safety reasons, high-intensity laser beams cannot be used. Signals were excluded from further analysis when the difference between the amplitudes during movement and during rest was smaller than 3 standard deviations of the signal during rest. The analysis was performed on the signals obtained from 10 subjects (the mean age was 28.1 years, ranging from 24 to 38 years, 5 females and 5 males).

### 2.2. *Experimental paradigm*

Subjects were placed in a supine position in a dark, electrically shielded room with their eyes closed in order to avoid blinking artifacts. The movement task involved tapping a computer mouse button with the right index finger after hearing an acoustic signal. The experimental session consisted of thirty 20-second periods of movement, each followed by a 30-second period of rest. At the end of the session, spontaneous activity was recorded for four minutes.

## 3. Experimental setup and preliminary signal analysis

### 3.1. *EEG*

EEG electrodes and fNIRS (functional Near Infrared Spectroscopy) optodes were fitted in a BioSemi cap. EEG activity was recorded from 32 active Ag/AgCl electrodes (BioSemi, 10/10 system) fitted over the frontal, central and posterior head structures. EEG was sampled at 4096 Hz, using a 24 bit A/D converter, down-sampled to 256 Hz after band-pass filtering from 3 to 47 Hz.

The Hjorth transform (a spatial Laplace filter approximation) was applied to the EEG signals. The epochs with artifacts were eliminated. The signals were zero-phase filtered (Butterworth, order 4) in the 8-13 Hz and 13-25 Hz bands for the extraction of alpha and beta rhythms respectively. The envelopes of the filtered time series were obtained as the instantaneous amplitude. The instantaneous amplitude was estimated as absolute value of the analytical signal by means of the Hilbert transform. The envelopes were high-pass filtered at a cutoff frequency of 0.02 Hz (Butterworth, order 4), and then the resulting signals were resampled at a frequency of 2 Hz.

### 3.2. *fNIRS*

The custom-made time-resolved fNIRS system[25] used in the study consisted of 2 laser light sources and 8 detectors. Two picosecond semiconductor laser diodes operating at the wavelengths of 687 nm and 832 nm generated light pulses at a frequency of 80 MHz. Those pulses were delivered to the healthy volunteer's head via 2-meter-long optical fibers. The light re-emitted from the tissue was transmitted to the detection module using 2-meter-long fiber bundles. The detection module consisted of eight photomultiplier tubes and eight time-correlated single photon counting cards. The source fibers and detecting bundles were placed on the subject's head between the EEG electrodes in such a way that their receptive fields corresponded to the electrodes: C3, C1, Cp3, Cp1 in the left hemisphere and symmetrically in the right hemisphere. The distance between the source fibers and the detecting bundles was 3.5 cm.

The distributions of Times of Flight of diffusely reflected photons (DTOFs) were recorded at two wavelengths in eight detection channels simultaneously. The analysis was based on the zeroth statistical moment of the DTOF (the total number of photons) and the first statistical moment of the DTOF (the mean time of flight of photons <t>). The mean path length of photons was calculated using <t> and the speed of light in the tissue assuming a refractive index n=1.4.[26] Based on the mean path length values and the relative changes in the total number of the detected photons obtained at both wavelengths, the changes in concentration of the oxyhemoglobin (HbO) and deoxyhemoglobin (HbR) were determined using the modified Beer-Lambert law and the wavelength-dependent molar extinction coefficients of hemoglobin.[27] The changes in the oxy- and deoxyhemoglobin concentrations were estimated based on fNIRS optical signals recorded with a sampling frequency of 10 Hz. Then the high-pass filter with cutoff frequency of 0.02 Hz (Butterworth, order 4) was applied and the signals were resampled at 2 Hz.

### 3.3. *ECG/HRV*

ECG signal was recorded at a sampling rate of 200 Hz from a three lead (RA, LL, RL) unipolar electrode

system called Finometer (Finapres Medical Systems BV). For detection of R peaks, we have applied an algorithm from the toolbox BioSig[28] based on the method proposed by Afonso[29] implemented in *nqrsdetect* procedure. The method relies on a filter bank which decomposes the ECG into subbands with uniform frequency bandwidths. Heart rate was obtained as a reciprocal of the time difference between two consecutive R waves in the ECG signal. Then, by means of a spline approximation the HRV signal was obtained. Similarly to the signals evaluated using EEG and fNIRS techniques, HRV was high pass filtered at 0.02 Hz and sampled at 2 Hz.

### 3.4. *BP*

Blood pressure was measured continuously from the left index finger by means of Finometer (Finapres Medical Systems BV). The signal was sampled at 200 Hz. Along with the positions of R waves, diastolic and systolic pressure values were obtained. Similarly to HRV, those time series were high pass filtered above 0.02 Hz and resampled at 2 Hz.

### 3.5. *Experimental conditions and types of analyzed signal epochs*

We considered three types of epochs in the current experiment:

(i) Signals coming from 20 s movement intervals are denoted by M. There were 30 M epochs per subject. Those epochs were synchronized with respect to the movement onset detected by pressing the button.
(ii) Signals taken from the last 20 s of the rest intervals between the movement periods are denoted by R. The first 10 s of the rest period were discarded to have the same epoch size under all conditions. There are 30 R epochs per subject.
(iii) Signals with a 20 s duration extracted from the 4 minutes of spontaneous activity recorded after the movement/rest session are denoted by S. 30 trials were obtained by shifting the 20 s window by 8 s.

## 4. Methods

### 4.1. *Estimation of connectivity*

The quantitative definition of causality formulated by Granger[22] is based on the predictability of time series. Thus, if a series $X_2(t)$ contains information in past terms that helps predict $X_1(t)$ and this information is contained in no other series used in the predictor, then $X_2(t)$ is said to cause $X_1(t)$. Formally, Granger causality can be expressed by the two-channel autoregressive (AR) model.[22]

The AR model can be generalized for an arbitrary number of channels. The Multichannel AR model (MVAR) for vector $X$ of $k$ signals recorded in time:

$X(t)=(X1(t), X2(t), ..., Xk(t))^T$ can be formulated in the following form[18]:

$$X(t) = \sum_{j=1}^{p} A(j)X(t-j) + E(t), \tag{1}$$

where $E(t)$ are the noise vectors of size $k$ and the coefficients $A$ are $k \times k$-sized matrices.

The MVAR transfer matrix is expressed by the model coefficients[18]:

$$H(f) = \left| \sum_{m=0}^{p} A(m) \exp(-2\pi i m f \Delta t) \right|. \tag{2}$$

Index m stands for the number of MVAR coefficient, $i$ stands for imaginary part. $H(f)$ contains information about frequency characteristics and relations between signals.[18]

Based on the properties of MVAR transfer function, Directed Transfer Function for an arbitrary number of channels may be defined[15]:

$$\mathrm{DTF}_{ji}(f) = \frac{\left|H_{ji}(f)\right|^2}{\sum_{m=1}^{k} \left|H_{im}(f)\right|^2}. \tag{3}$$

DTF describes causal influence of channel $j$ on channel $i$ at frequency $f$. DTF is a frequency dependent causal measure of interdependence between signals. It was shown[30] that DTF is proportional to the coupling between the time series, so using DTF, we can find the coupling strength in a given frequency band. In the Eq. (3) the denominator is dependent on frequency, so the spectral characteristic of DTF depends on the frequency properties of all the EEG channels, not only of the considered channel. To avoid this influence, the ffDTF function was introduced.[31] In ffDTF, the denominator is integrated over frequencies, so the spectrum of the estimator ffDTF is not influenced by the frequency characteristics of the normalizing factor in the denominator.[31]

$$\mathrm{ffDTF}_{ji}(f) = \frac{\left|H_{ji}(f)\right|^2}{\sum_f \sum_{m=1}^{k} \left|H_{im}(f)\right|^2}, \qquad (4)$$

ffDTF, like DTF, takes values in the range [0, 1]. In our calculations we applied the ffDTF function.

MVAR is a parametric model and the number of its parameters should preferably be at least ten times smaller than the number of data points. When short realizations are only available, as was the case in our finger movement task, multiple repetitions of the experiment may be used for the ensemble averaging in the model fitting procedure.[17,30] The determination of the model coefficients is based on the estimation of the correlation matrix $R_{ij}$. For each trial (realization) indexed by (r) we calculate the correlation matrix $R_{ij}(r)$. Then we average these correlation matrices over the $N_T$ realizations. The resulting model coefficients are based on the ensemble averaged correlation matrix:

$$\tilde{R}_{ij}(s) = \frac{1}{N_T} \sum_{r=1}^{N_T} R_{ij}^{(r)}(s) =$$

$$= \frac{1}{N_T} \sum_{r=1}^{N_T} \frac{1}{N_S} \sum_{t=1}^{N_S} X_i^{(r)}(t) X_j^{(r)}(t+s), \qquad (5)$$

where $N_T$– number of realizations, $N_S$– number of data points in the window, $r$ – index of realization.

The incorporation of the information from all the repetitions of the experiment into one model enhances the common features of the signals, which results in an increase in the statistical significance of the results.

All the seven signals: (1) systolic (sBP) and (2) diastolic (dBP) blood pressure, (3) heart rate variability (HRV), changes in concentration of (4) oxygenated (HbO) and (5) deoxygenated (HbR) hemoglobin, (6) EEG alpha rhythm amplitude envelopes (EEG alpha) and (7) EEG beta rhythm amplitude envelopes (EEG beta) served as the input for the MVAR model. The EEG signals from the C3 electrode (overlying the motor cortex of the moving finger) and the signals obtained from the corresponding fNIRS optode were analyzed. To quantify the coupling in the LFO range, we use a ffDTF integral in the range of 0.05 – 0.15 Hz, denoted by $C_{ji}$.

### 4.2. *Statistical analysis*

The theoretical distribution of $C_{ji}$ is unknown; therefore, we based statistical inference on the comparisons of its values with the distributions of the corresponding values obtained for surrogate data, (the data with randomized phases) or by means of bootstrap, depending on the type of test. We performed two types of tests. The first type is designed to test the significance of the network couplings present in each type of epochs (M, R or S).

Thus, given a type of epoch, the hypotheses were:

$$\text{H0: } \left[C_{ji}\right]_{sub} = \left[C_{ji}^{surr}\right]_{sub},$$

$$\text{H1: } \left[C_{ji}\right]_{sub} > \left[C_{ji}^{surr}\right]_{sub},$$

where $[\cdot]_{sub}$ means the estimates averaged over subjects, $C_{ji}$ was estimated for the original data for a given subject, and was estimated for the surrogate data of a given subject.

The surrogate data were obtained in the usual way, by transforming the signals to the frequency domain using FFT, randomizing the phases and performing the inverse transform. The process of surrogate data generation and $C_{ji}^{surr}$ estimation was performed 1000 times for each subject. The estimates obtained in this way were averaged over subjects. The set of 1000 $\left[C_{ji}^{surr}\right]_{sub}$ yielded the null hypothesis distribution. The probability of type I error was obtained as the fraction of the distribution greater than the $\left[C_{ji}\right]_{sub}$, i.e. observed for the original data. Since we performed a family of 42 tests (combinations of 7 signals) to account for the multiple comparisons, those probabilities were further corrected by the FDR method.[32]

The second type of test was designed to detect possible differences in the connectivity between the pairs of epochs: M vs. R, and M vs. S. In this case, we used the bootstrap paired test. The hypotheses were:

H0: $D = 0$ , and alternatively

H1: $D \neq 0$ ,

where $D = [\Delta_{ji}]_{sub}$ , $\Delta_{ji}$ – averaged across subjects, and $\Delta_{ji} = C_{ji}^{type1} - C_{ji}^{type2}$ is the within-subject difference in the $ji$ connection. Here, $C_{ji}^{type1}$ is the connectivity estimated for the M epochs, and $C_{ji}^{type2}$ is the connectivity estimated for the R or S types of epoch.

The distribution of $D$ corresponding to the null hypothesis was obtained in the following bootstrap procedure:

1. For a given subject, create a pool of type1 and type2 trials (in our case of type: S, R or M) and then apply the following procedure:

   1.1. Randomly select a subset of 30 trials to be marked as type1,
   1.2. Randomly select a subset of another 30 trials to be marked as type2,
   1.3. Compute $\Delta_{ji}^{boot} = C_{ji}^{type1} - C_{ji}^{type2}$,

2. Average $\Delta_{ji}^{boot}$ across subjects to obtain $D_{boot} = \left\lfloor \Delta_{ji}^{boot} \right\rfloor_{sub}$,

3. Repeat steps 1) - 2) N = 1000 times.

The H1 is two-sided, and thus the probability of type I error was obtained as the fraction of the bootstrap distribution satisfying $|D_{boot}| > |D|$, i.e. more extreme than observed for the original data labelling. Since we performed a family of 42 tests to account for the multiple comparisons, those probabilities were further corrected by the FDR (false discovery rate) method.[32]

## 5. Results

MVAR model was fitted to all the considered signals: systolic and diastolic blood pressure, heart rate variability, changes in concentration of blood oxygenation and deoxygenation, and amplitude envelopes of EEG alpha and beta rhythms, and then ffDTFs were estimated according to the Eq. (4). The ffDTFs calculated for spontaneous activity (the S epochs) averaged over subjects are shown in Fig.1. Peaks at frequencies around 0.1 Hz (LFO) and 0.4 Hz can be distinguished. The striking feature visible in Fig. 1 is the high values of ffDTF functions showing influence of the sBP, dBP and HRV variables on the other variables. The spectral peaks in ffDTFs at about

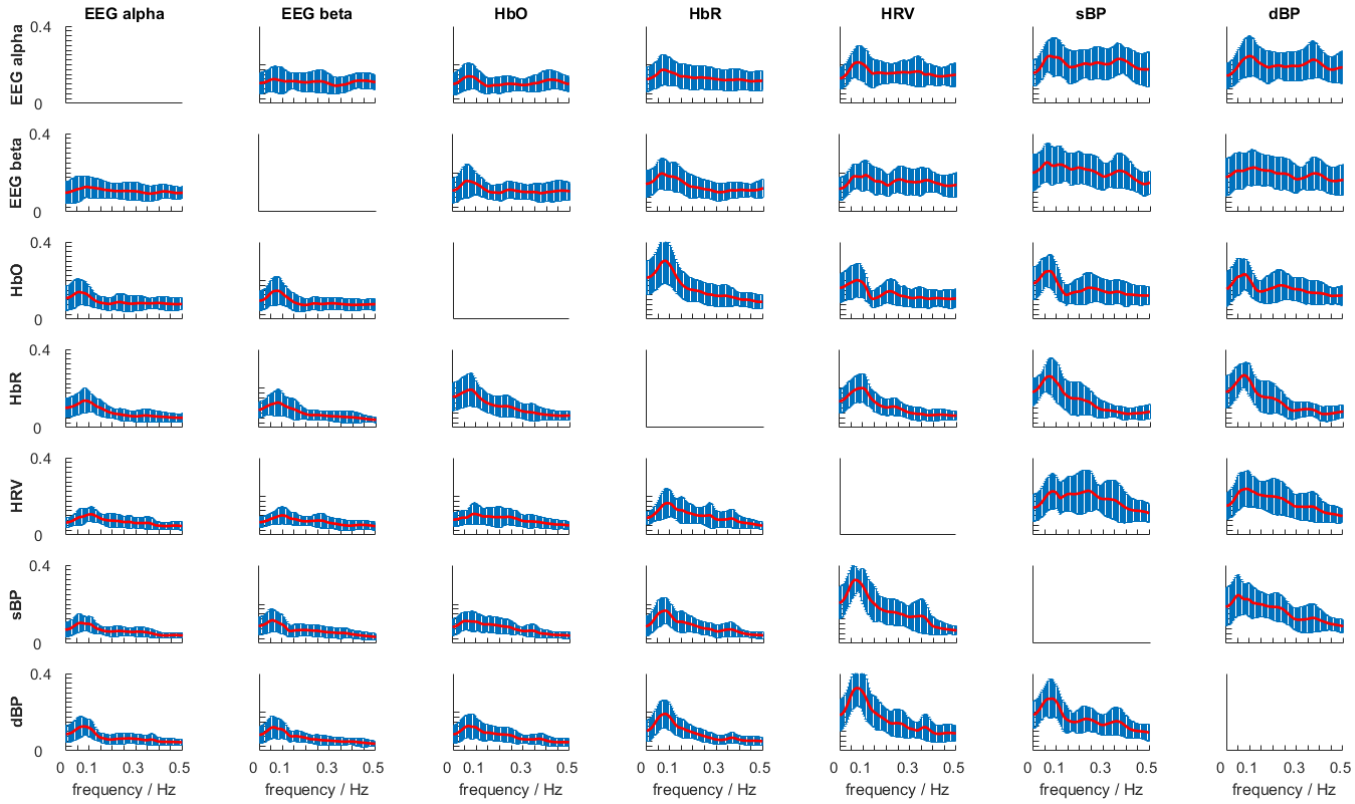


Fig.1. ffDTFs for spontaneous activity averaged over subjects plotted as a function of frequency. The direction of couplings from the variable marked below the column to the variable marked on the left . The standard deviations are marked. The square roots of ffDTFs were plotted for better visualization.

0.1 Hz were most prominent for those variables. The spectral peaks at 0.1 for HbR showed a strong influence of this signal on HbO and also, to somehow a lesser degree, on sBP and dBP. According to the literature[33], we can assume that the peak at about 0.4 Hz is connected with respiration. For different subjects the maxima of LFO peaks had different positions, so for averaged ffDTFs the peak was not always very distinct.

The ffDTF integrals, called $C_{ji}$, representing the strength of coupling between sBP, dBP, HRV, HbO, HbR, EEG alpha and EEG beta in the LFOs frequency range (0.05–0.15 Hz), were computed together with their significances in accordance with the procedures described in Section 4.2.

The values of the couplings during spontaneous activity are presented in Table 1, and a graph illustrating the obtained causal relationships is shown in Fig. 2. The prominent features of interactions are strong reciprocal couplings between sBP and dBP, where the influence of sBP on dBP is stronger than vice versa. Reciprocal connections of comparable strengths are also prominent between sBP and dBP and HRV. This kind of interaction indicates the existence of feedback loops. The directed connections from EEG alpha and EEG beta toward the other variables are much weaker.

Table 1. The averaged strengths of couplings in the range of 0.05-0.15 Hz for spontaneous activity. The significant interactions are printed in bold on a gray background. FDR is controlled at the 5% level. The direction of interaction from the variable marked below the column to the variable marked on the left.

| | | | | | | | |
|---|---|---|---|---|---|---|---|
| EEG Alpha | | **0.30** | 0.32 | **0.54** | **0.78** | **1.11** | **1.05** |
| EEG Beta | **0.31** | | **0.42** | **0.70** | **0.67** | **1.22** | **0.99** |
| HbO | **0.30** | **0.35** | | **1.47** | **0.61** | **0.86** | **0.80** |
| HbR | **0.32** | **0.27** | **0.61** | | **0.71** | **1.09** | **1.12** |
| HRV | **0.20** | 0.18 | 0.21 | **0.46** | | **0.92** | **1.05** |
| sBP | 0.19 | 0.19 | 0.25 | **0.43** | **1.69** | | **1.04** |
| dBP | **0.25** | **0.23** | 0.28 | **0.56** | **1.70** | **1.19** | |
| | EEG Alpha | EEG Beta | HbO | HbR | HRV | sBP | dBP |

Table 2. The averaged strengths of couplings in the range of 0.05-0.15 Hz for rest activity. The significant interactions are printed in bold on a gray background. FDR is controlled at the 5% level. The direction of interaction from the variable marked below the column to the variable marked on the left.

| | | | | | | | |
|---|---|---|---|---|---|---|---|
| EEG Alpha | | **0.43** | 0.36 | **0.54** | 0.55 | **0.93** | **0.81** |
| EEG Beta | 0.23 | | 0.34 | 0.46 | **0.56** | **0.88** | **0.89** |
| HbO | 0.22 | 0.27 | | **1.45** | **0.61** | **0.82** | **0.89** |
| HbR | 0.21 | 0.25 | **0.58** | | **0.53** | **0.69** | **0.70** |
| HRV | 0.13 | 0.14 | 0.17 | 0.26 | | **0.63** | **1.15** |
| sBP | 0.12 | 0.13 | 0.20 | 0.29 | **1.74** | | **1.04** |
| dBP | 0.13 | 0.14 | 0.20 | 0.33 | **1.75** | **0.87** | |
| | EEG Alpha | EEG Beta | HbO | HbR | HRV | sBP | dBP |

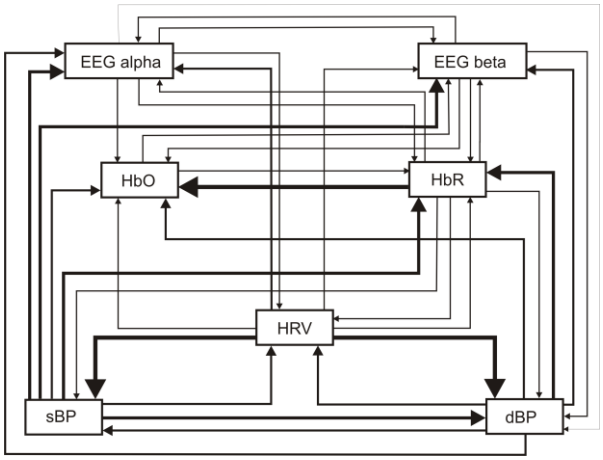


Fig. 2. Scheme showing significant couplings for spontaneous activity calculated using the approach described in Section 4.2. The thickness of the arrows represents the strength of connections. The thickest lines (relative thickness 4) denote the coupling values greater than 1.42, the next thicknesses correspond to the values in the ranges of 1.09 – 1.42, 1.08-0.75 and below 0.75. For the exact values of couplings refer to Table 1.

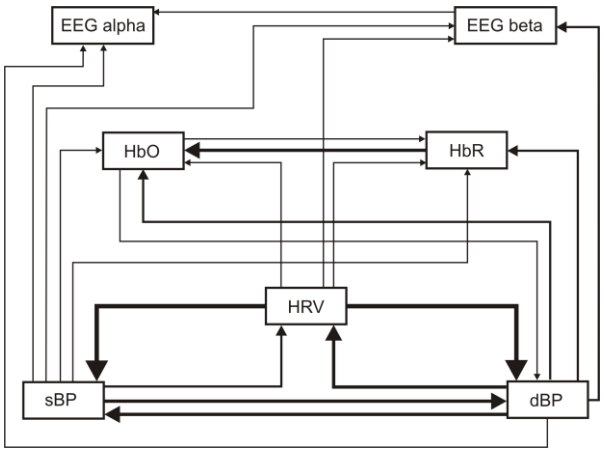


Fig.3 Scheme showing significant strengths of couplings for movement calculated using the approach described in Section 4.2. The thickness of the arrows represents the strength of connections. The thickest lines (relative thickness 4) denote the coupling values greater than 1.42, the next thicknesses correspond to the values in the ranges of 1.09 – 1.42, 1.08-0.75 and below 0.75. For the exact values of couplings refer to Table 3.

Inspecting the graph, it is easy to notice that sBP and dBP drive HbO , HbR, EEG alpha and EEG beta. The HRV signal also exerts an influence on EEG alpha and EEG beta. The influence of HbR on EEG alpha and EEG beta is stronger than the influence of HbO. HbO and HbR are connected reciprocally; however, the influence of HbR on HbO is much stronger than vice versa.

The values of couplings for the R and M periods are shown respectively in Tables 2 and 3. For the R periods, the overall scheme of couplings is more similar to the one obtained in the M condition than in the S one . In particular, the influence of EEG alpha and EEG beta on the other variables became insignificant. The pattern of connections for the M period is illustrated in Fig. 3.

Next, we compared the paired coupling changes in LFO between the M and R epochs, and then between the M and S epochs. Practically no significant differences in the couplings between the M and R epochs were found; however, some significant differences were found between the M and S epochs (Table 4 and Fig. 4).

## 6. Discussion

Several authors have studied the relationship between vascular, hemodynamic and electrophysiological signals in the LFO range; however, their studies were based on bivariate methods which considered only two signals at a time.

E.g. Nikulin et al.[14] investigated the relationships between ultra-slow (0.07-0.14 Hz) oscillations (MUSO) occurring in EEG and metabolic variables. The authors reported positive coherences between MUSO, HbO levels and blood pressure during rest and when a subject was kept in a tilted position. They suggested an extra-neuronal origin of MUSO reflecting cerebral vasomotion.

The works of particular interest in the context of our results are those where directional interactions between metabolic and electrophysiological signals were considered. Obrig et al.[6] investigated spontaneous low frequency oscillations in the visual cortex. The authors reported that HbR changes preceded HbO oscillations, which is in agreement with our results (Fig.2 and Fig.3) showing a stronger influence of HbR on HbO than vice versa. In that work positive coherence between arterial BP (aBP) and HbO and HbR was also observed. Directional interaction between aBP and HbR (aBP

preceding HbR) was found; however, no influence of aBP on HbO was reported.

Pfurtscheller et al.[9] studied LFO around 0.1 Hz in cardiovascular and cerebral systems for spontaneous activity and during finger movement. For spontaneous activity, phase shifts between dBP and HRV varied depending on subject, but BP was always leading. During movement the phase shifts increased and became even more variable. Also, dBP temporarily preceded prefrontal HbO concentration levels.

In Ref. 10 coupling between EEG and hemodynamic signals during rest and movement was considered. Cross-spectral analysis and time-frequency methods were applied. Large inter-subject variability was observed. The reported results indicated that the positive HbO peaks preceded the central EEG beta and alpha power in the majority of subjects. During voluntary movements the results were similar and HbO peaks preceded EEG power maxima; however, the phase shifts between the signals were smaller.

Table 3. The averaged strengths of couplings in the range of 0.05-0.15 Hz for movement activity. The significant interactions are printed in bold on a gray background. FDR is controlled at the 5% level. The direction of interaction from the variable marked below the column to the variable marked on the left.

| EEG Alpha | | **0.28** | 0.31 | 0.42 | 0.44 | **0.72** | **0.71** |
|---|---|---|---|---|---|---|---|
| EEG Beta | 0.18 | | 0.38 | 0.48 | **0.59** | **0.73** | **0.78** |
| HbO | 0.16 | 0.21 | | **1.39** | **0.58** | **0.73** | **0.89** |
| HbR | 0.15 | 0.16 | **0.68** | | **0.57** | **0.66** | **0.80** |
| HRV | 0.10 | 0.13 | 0.25 | 0.24 | | **0.84** | **1.15** |
| sBP | 0.12 | 0.12 | 0.27 | 0.32 | **1.62** | | **1.16** |
| dBP | 0.14 | 0.14 | **0.31** | 0.34 | **1.59** | **1.09** | |
| | EEG Alpha | EEG Beta | HbO | HbR | HRV | sBP | dBP |

Table 4. The differences in the couplings between movement and spontaneous activity. The significant differences are printed in bold. The couplings that were significant for spontaneous activity are marked with a gray background. FDR is controlled at the 5% level.

| EEG Alpha | | -0.02 | -0.01 | -0.12 | **-0.34** | **-0.39** | **-0.34** |
|---|---|---|---|---|---|---|---|
| EEG Beta | **-0.13** | | -0.04 | **-0.21** | -0.08 | **-0.49** | -0.21 |
| HbO | **-0.14** | **-0.13** | | -0.08 | -0.03 | -0.14 | 0.09 |
| HbR | **-0.17** | **-0.11** | 0.07 | | -0.14 | **-0.43** | -0.32 |
| HRV | **-0.09** | -0.05 | 0.04 | **-0.21** | | -0.08 | 0.10 |
| sBP | -0.07 | -0.07 | 0.02 | -0.11 | -0.08 | | 0.13 |
| dBP | **-0.11** | **-0.09** | 0.03 | **-0.22** | -0.11 | -0.10 | |
| | EEG Alpha | EEG Beta | HbO | HbR | HRV | sBP | dBP |

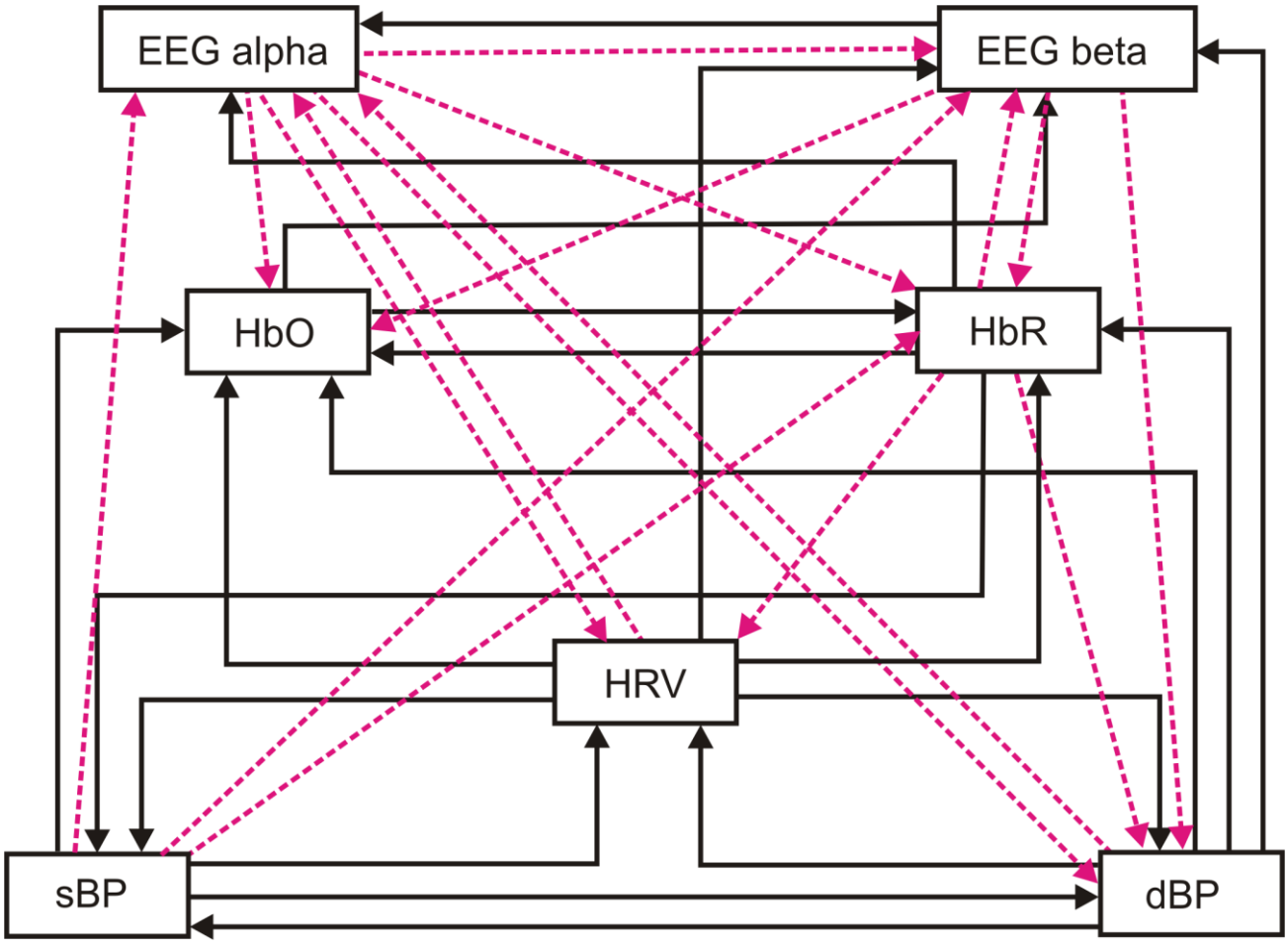


Fig.4 Scheme showing changes of couplings between movement and spontaneous activity. The solid lines represent the couplings that did not change significantly with respect to spontaneous activity and the red dashed lines denote the couplings that significantly decreased during movement. For the values of changes in the couplings refer to Table 4.

Summarizing the present literature, we can state that the reported results correspond well with ours in respect of directionality of interactions; however, they only concern fragmentary relationships between signals. The formalism applied in them did not allow identification of reciprocal connections and above all, it was unable to grasp the whole scheme of interactions between the relevant time series.

Considering the pattern of connections for the spontaneous activity, the most prominent feature is driving oscillations in HbO and HbR concentration as well as EEG alfa and EEG beta by blood pressure. Indeed, MW were first identified as oscillations of BP and they are considered to be systemic fluctuations due to the vascular autoregulation dynamics.

The MW generation mechanisms are in dispute. One of the proposed mechanisms assumes the autonomous oscillator located either in the brainstem or in the spinal cord. The other proposed mechanism concerns the action of the baroreflex loop.[11] Our results support the second hypothesis. The remarkable feature of the connections between BP and HRV is a strong reciprocal coupling between those signals. The identified network encompassing sBP, dBP and HRV appears to be an important structure in generation of MW and seems to act as an autoregulation system to initiate cardiac autonomic adjustments. The specificity of connectivity between HRV and BP does not support the hypothesis that heart rate oscillations buffer Mayer waves[11] rather than reinforce them.

MW connected with blood pressure oscillations seem to be the primary cause of amplitude fluctuations of alpha and beta rhythms as well as the changes in concentrations of HbO and HbR. Considering the

coupling between HbO and HbR, we can observe a stronger influence of HbR on HbO than vice versa. It seems logical that the rise in deoxygenated hemoglobin will in turn cause an increase in HbO. This increase may be possibly due to the influence of HRV since according to our results this variable is coupled to HbO and HbR.

The scheme of connections during movement does not vary practically with respect to the one observed for rest (Table 2) This observation is not surprising. Functionally, the state of subjects during rest periods when they are attentive and anticipating stimulus is quite different from their state during longer periods of spontaneous activity. During short periods of rest, the activity of the system is not stable enough to allow the development of the type of patterns with strong couplings between all the variables observed during longer periods of spontaneous activity. The movement comes as a perturbation of the spontaneous system and causes breaking or weakening of the bonds between the variables. Those bonds are not reconstructed during short periods of rest. The signals changes during movement with respect to rest involve a slow rise in HbO, a decrease in HbR (which lasted about 25 s) and a desynchronization of EEG alpha and EEG beta. These phenomena described in Ref. 34 have spectral characteristics below the MW frequency range which we are considering here, so they are not reflected in the present results. The slow evolution of HbO and HbR and amplitudes of EEG alpha and EEG beta in rest and movements periods were modulated by oscillations of frequency around 0.1 Hz, similarly for both conditions therefore it is not surprising that when oscillating activity is considered the differences are hardly observed.

The differences between spontaneous activity and movement are shown in Table 4 and illustrated in Fig.4. Most of the couplings observed for spontaneous activity can be observed also during movement. The sBP, dBP and HRV are connected by strong reciprocal bonds. Changing the coupling pattern from S to M causes weakening or breaking of certain connections. The influence of EEG alpha and EEG beta on the other variables which were not strong even during spontaneous activity disappears. This can be explained by the effect of desynchronization of those rhythms during movement. The driving of EEG alpha fluctuations by dBP and sBP is significantly reduced. There is also a decrease in the influence of HbR on HRV. However the influence of HRV on HbR stays on the same level during movement and spontaneous activity. A decrease in the influence of sBP oscillations during movement on EEG alpha, EEG beta and HbR is understandable since the intrinsic oscillations in the resting system are usually suppressed by external perturbations. Another interesting result of our study is the identification of strong reciprocal couplings between sBP, dBP and HRV constituting a circuit which is acting during spontaneous and movement activity.

We considered several variables involved in the control of brain-heart autoregulatory mechanism. However, the system is highly complex and there are other variables not recorded by us which possibly have to be taken into account. In particular, information about sympathetic nerve activity (difficult to measure in humans) would be beneficial for understanding MW generation mechanisms since neurovascular signals are under the control of the autonomic nervous system, especially the efferent sympathetic system (including baroreceptors) which modulates circulatory and hemodynamic variables.[33]

An important aspect which has to be taken into account is the fact that our experimental design did not allow the recording of signals from subcortical structures that cannot be probed by the NIRS technique and might possibly influence the relationships between the investigated variables. The functional magnetic resonance technique (fMRI) allows the study of neurovascular couplings also in subcortical brain structures. Recently, some valuable contributions concerning the blood oxygenation level-dependent (BOLD) signals have been considered in the aspect of LFO in the 0.1 Hz range. [12,13,35,36]

Tong et al.[36] found a strong correlation between LFOs measured at the periphery by the NIRS technique with the BOLD signals and suggested a global circulatory origin of LFOs in the human brain. They postulated that the resting state networks may to some extent reflect vascular anatomy associated with systemic LFOs, rather than neuronal connectivity.

On the other hand, the works[12,13] aimed at finding the distinction between neural and vascular BOLD oscillations. In[12] by means of phase locking index, for oscillations at around 0.1 Hz in BOLD signals time delays were found between the precentral gyrus (PCG) and insula for rest and movement. About half of the participants revealed in PCG time delays distinctive for

neural BOLD oscillations. In the resting state they were significantly associated with ~0.1 Hz heart rate variability.

Two clusters of phase coupling between the slow BOLD oscillations at 0.1 Hz and the heart rate interval oscillations in the midcingulum were found, one representative of neural and the other of vascular BOLD oscillations.[13] The results of the above publications indicate the influence of the "central pacemaker" oscillations on HRV.

Our results provided a comprehensive scheme of interactions between electrical brain and heart signals, hemodynamic variables and blood pressure oscillations. We demonstrated that in the frequency range around 0.1 Hz HRV, sBP and dBP signals are tightly coupled by reciprocal connections which may lead to the observed oscillatory behavior; however, the mechanisms of 0.1 Hz oscillations may be influenced by the cerebral structures. Further research is needed for elucidation the possible role of brain structures in MW generation.

We may conclude that the generation and propagation of the MW in the cardiovascular and neurovascular systems result from the complex mechanisms of vascular and neural origin involving several mutually interacting variables.

## Aknowledgments

This work was supported by NCN grant Nr. 2014/15/B/ST7/0526

## References

1. Mayer S. Studien zur Physiologie des Herzens und der Blutgefässe 6. Abhandlung: Über spontane Blutdruckschwankungen. Sitzungsberichte Akad der Wissenschaften Wien Math Classe, Anat. 1876;74:281–307.
2. Cerutti C, Barres C, Paultre C. Baroreflex modulation of blood pressure and heart rate variabilities in rats: assessment by spectral analysis. Am J Physiol. 1994;266(5 Pt 2):H1993–2000.
3. Cevese A, Gulli G, Polati E, Gottin L, Grasso R. Baroreflex and oscillation of heart period at 0.1 Hz studied by α-blockade and cross-spectral analysis in healthy humans. J Physiol. Wiley-Blackwell; 2001;531(1):235–44.
4. Draghici AE, Taylor JA. The physiological basis and measurement of heart rate variability in humans. J Physiol Anthropol. BioMed Central; 2016 Sep 28;35(1):22.
5. Hoshi Y, Tamura M. Dynamic changes in cerebral oxygenation in chemically induced seizures in rats: study by near-infrared spectrophotometry. Brain Res. 1993;603(2):215–21.
6. Obrig H, Neufang M, Wenzel R, Kohl M, Steinbrink J, Einhäupl K, et al. Spontaneous Low Frequency Oscillations of Cerebral Hemodynamics and Metabolism in Human Adults. Neuroimage. 2000;12(6):623–39.
7. Yücel MA, Selb J, Aasted CM, Lin P-Y, Borsook D, Becerra L, et al. Mayer waves reduce the accuracy of estimated hemodynamic response functions in functional near-infrared spectroscopy. Biomed Opt Express. 2016;7(8):3078–88.
8. Achermann P, Borbély AA. Low-frequency (< 1 hz) oscillations in the human sleep electroencephalogram. Neuroscience. Pergamon; 1997 Aug 26 81(1):213–22.
9. Pfurtscheller G, Klobassa DS, Altstatter C, Bauernfeind G, Neuper C. About the stability of phase shifts between slow oscillations around 0.1 Hz in cardiovascular and cerebral systems. IEEE Trans Biomed Eng. 2011;58(7):2064–71.
10. Pfurtscheller G, Daly I, Bauernfeind G, Müller-Putz GR. Coupling between intrinsic prefrontal Hbo2 and central EEG beta power oscillations in the resting brain. Zang Y-F, editor. PLoS One. Public Library of Science; 2012;7(8):e43640.
11. Julien C. The enigma of Mayer waves: Facts and models. Cardiovascular Research. Oxford University Press; 2006. p. 12–21.
12. Pfurtscheller, G., Schwerdtfeger A., Brunner C., Aigner C., Fink D., Brito J., Carmo M.P., Andrade A. (2017a). "Distinction between Neural and Vascular BOLD Oscillations and Intertwined Heart Rate Oscillations at 0.1 Hz in the Resting State and during Movement." PLoS One 12(1): e0168097.
13. Pfurtscheller, G., Schwerdtfeger A., Srither-Presler A., Brunner C., Aigner C., Brito J., Carmo M.P., Andrade A . (2017b). "Brain-heart communication: Evidence for "central pacemaker" oscillations with a dominant frequency at 0.1Hz in the cingulum." Clin Neurophysiol 128(1): 183-193.
14. Nikulin V V., Fedele T, Mehnert J, Lipp A, Noack C, Steinbrink J, et al. Monochromatic Ultra-Slow (~0.1Hz) Oscillations in the human electroencephalogram and their relation to hemodynamics. Neuroimage. 2014;97:71–80.
15. Kaminski MJ, Blinowska KJ. A new method of the description of the information flow in the brain structures. Biol Cybern. Springer-Verlag; 1991;65(3):203–10.
16. Winterhalder M., Schelter B., Hesse W., Schawab K., Leistritz L., Klan D., Bauer R, Timmer J., Witte H. Comparison of linear signal processing techniques to infer directed interactons in multivariate neural systems. Signal Processing (2005) 85: 2137-2160.
17. Blinowska KJ. Review of the methods of determination of directed connectivity from multichannel data. Medical and Biological Engineering and Computing. Springer; 2011. p. 521–9.

18. Blinowska, K.J. and Zygierewicz, J.; Practical Biomedical Analysis using Matlab. CRC press Taylor and Francis Group, Boca Raton, London, New York, 2012.
19. Pereda E, Quiroga RQ, Bhattacharya J (2005) Nonlinear multivariate analysis of neurophysiological signals. Prog Neurobiol. 77:1-37.
20. Blinowska KJ, Kuś R, Kamiński M. Granger causality and information flow in multivariate processes. Phys Rev E - Stat Nonlinear, Soft Matter Phys. 2004;70(5 1):50902
21. Blinowska KJ, Kaminski M. Functional Brain Networks: Random, "Small World" or Deterministic? PLoS One. Public Library of Science (PLoS); 2013;8(10):e78763.
22. Granger CWJ. Investigating Causal Relations by Econometric Models and Cross-spectral Methods. Econometrica. The Econometric Society; 1969;37(3):424.
23. Mima T, Matsuoka T, Hallett M. Information flow from the sensorimotor cortex to muscle in humans. Clin Neurophysiol. 2001;112(1):122–6.
24. Sawosz, P., et al., Human skull translucency: post mortem studies. Biomed Opt Express, 2016. 7(12): p. 5010-5020.
25. Kacprzak M., Liebert A., Staszkiewicz W., Gabrusiewicz A., Sawosz P., Madycki G., and Maniewski R., Application of a time-resolved optical brain imager for monitoring cerebral oxygenation during carotid surgery. J Biomed Opt, 2012. 17(1): p. 016002.
26. Jacques SL. Optical properties of biological tissues: a review. Phys Med Biol. IOP Publishing; 2013 Jun 7;58(11):R37–61
27. Prahl, S. A. Tabulated molar extinction coefficient for hemoglobin in water. http//omlc. ogi. edu/spectra/hemoglobin/summary. html (1999)
28. Vidaurre C, Sander T, Schlögl A. BioSig: The Free and Open Source Software Library for Biomedical Signal Processing. March 2011 Computational Intelligence and Neuroscience 2011(5):935364
29. V. Afonso, W. Tompkins, T. Nguyen, and S. Luo, "ECG beat detection using filter banks," IEEE Trans. Biomed. Eng., vol. 46, no. 2, pp. 192-202, Feb. 1999
30. Kamiński M, Ding M, Truccolo WA, Bressler SL. Evaluating causal relations in neural systems: Granger causality, directed transfer function and statistical assessment of significance. Biol Cybern. Springer-Verlag; 2001;85(2):145–57.
31. Korzeniewska A, Mańczak M, Kamiński M, Blinowska KJ, Kasicki S. Determination of information flow direction among brain structures by a modified directed transfer function (dDTF) method. J Neurosci Methods. Elsevier; 2003;125(1–2):195–207.
32. Benjamini, Yoav; Hochberg, Yosef (1995). "Controlling the false discovery rate: a practical and powerful approach to multiple testing". Journal of the Royal Statistical Society, Series B. 57 (1): 289–300. MR 1325392
33. Malliani A, Pagani M, Lombardi F, Cerutti S. Cardiovascular neural regulation explored in the frequency domain. Circulation. 1991;84(2):482–92
34. Lachert, P.,Janusek D, Pulawski P., Milej D., Liebert A., Blinowska K.J.. (2017). "Coupling of Oxy- and Deoxyhemoglobin concentrations with EEG rhythms during motor task." Sci Rep 7(1): 15414.
35. Pfurtscheller G, Bauernfeind G, Neuper C, Lopes da Silva FH. Does conscious intention to perform a motor act depend on slow prefrontal (de)oxyhemoglobin oscillations in the resting brain? Neurosci Lett. 2012;508(2):89–94.
36. Tong, Y. J.,Hocke L.M., Fan X., Janes A.,C., Frederick B.. (2015). "Can apparent resting state connectivity arise from systemic fluctuations?" Frontiers in Human Neuroscience 9:285.